

Spectral Analysis of HIV Drugs for Acquired Immunodeficiency Syndrome Within Modified Non-invasive Methods

RAOUL R. NIGMATULLIN¹, DUMITRU BALEANU^{2,3,4}, ABDULRAHIM A. AL-ZHRANI³, YAHIA A. ALHAMED³, ADNAN H. ZAHID³, TAMER E. YOUSSEF^{3,5}

¹Theoretical Physics Department, Institute of Physics, Kazan Federal University, Kremlevskaya str.18, 420008, Kazan, Russia

²Department of Mathematics and Computer Sciences, Faculty of Arts and Sciences, Cankaya University, TR-06530 Ankara, Turkey

³Chemical and Materials Engineering Department, Faculty of Engineering, King Abdulaziz University, P. O. Box 80204, Jeddah, 21589, Saudi Arabia

⁴Institute of Space Sciences, Magurele, RO-077125 Bucharest, Romania

⁵Applied Organic Chemistry Department, National Research Center, Dokki, Cairo, 12622, Egypt

In this study a chromatographic separation of active ingredients for four drugs namely Combivir, Kaletra, Valcyte and Viramune was performed on thin layer chromatography (TLC). Their spectra were analyzed for acquired immunodeficiency syndrome by using the Fourier transform infrared spectroscopy spectra combined with the new procedure of the optimal linear smoothing. Fourier transform of the second type was applied as the fitting function based on some significant set of frequencies for the smoothed signals. The obtained results show that the proposed method is efficient and easy to apply in extracting of a hidden information from signals corresponding to the four investigated drugs.

Keywords: chromatographic separation, Valganciclovir, Nevirapine, Lopinavir, Ritonavir, Lamivudine, Zidovudine, Fourier transform infrared spectroscopy

The science of complexity is a fascinating field of study due to the fact that it provides a new view of many real phenomena which in the last decades have seemed to be inexplicable, suggesting an interesting interpretation of the reality. During the last few years new methods and techniques were applied to extract hidden properties of the dynamics of complex systems [1-7].

There are approximately more than 33 million people currently infected with the human immunodeficiency virus (HIV), the causative agent of acquired immunodeficiency syndrome (AIDS), making this one of the major public health problems worldwide [8]. Due to the fact that HIV develops resistance rapidly [9], new therapeutic strategy of AIDS treatment requires a combination containing two or more anti-HIV active compounds. Such a combination dosage form will be adhering to effective therapy and enhancing better patient compliance.

In recent decades, a high effective therapy for acquired immunodeficiency syndrome (AIDS) was obtained by using commercial complex mixtures comprising different combinations of several anti-HIV drugs including nucleoside reverse transcriptase inhibitors and non-nucleoside reverse transcriptase inhibitors or protease inhibitors.

As it is known Combivir [10] and Kaletra [11] are an HIV medication. They are in a category of HIV medicines called nucleoside reverse transcriptase inhibitors (NRTIs) and protease inhibitors (PIs), respectively. They prevent HIV by increasing the number of CD4 cells, which prevent the cells from producing new virus and decrease the amount of virus in the body.

Valcyte [12] and Nevirapine [13] are showing a potent and synergistic effect on inhibition of the human immunodeficiency virus (HIV-1). Valcyte has been used for the treatment of CMV retinitis in patients with weakened immune systems but Nevirapine used in the 'highly active antiretroviral treatment' or HAART which is considered as

one of the most significant advances in the field of HIV therapy [14].

Therefore, new methods and techniques should be invented to extract more information, with the Fourier transform infrared spectroscopy (FTIR), from the spectra of drugs for acquired immunodeficiency syndrome.

The main aim of this manuscript is to propose a new technique to deal with the FTIR spectra of Combivir, Kaletra, Valcyte and Viramune.

The organization of the manuscript is as follows:

Section 1 deals with sample solution preparation of drugs and chromatographic separation of their active ingredients. After that we discuss the application of the new procedure of optimal smoothing for four drug spectra corresponding to Combivir, Kaletra, Valcyte and Viramune. In the next step the Fourier transform of the second type was applied in order to characterize the investigated spectra. Finally, we present our conclusions.

Experimental part

Materials and methods

Combivir was kindly provided by GlaxoSmithKline; Kaletra by Abbott; Viramune by Boehringer Ingelheim and Valcyte by Roche. Analytical grade methanol (BDH, England), analytical grade chloroform (Sigma-Aldrich, Germany), analytical grade *n*-hexane (BDH, England) were also used during the method development.

Sample solution preparation

Twenty tablets of Combivir: (containing 150 mg of Lamivudine and 300 mg of Zidovudine) or Kaletra: (containing 200 mg of Lopinavir and 50 mg of Ritonavir) were accurately weighed and powdered. A portion of the powder equivalent to 75 mg of Lamivudine and 150 mg of Zidovudine (Combivir) or 100 mg of Lopinavir and 25 mg of Ritonavir (Kaletra) was weighed and quantitatively transferred into a 100 mL volumetric flask. The powder

*email: dumitru@cankaya.edu.tr; Tel.: +90 312 2331424

was dissolved using Ethanol with the aid of mechanical shaking for 15 min and sonication for 30 min for separating out the insoluble materials and binding agents. A sample solution of 25 mL of the stock solution was transferred into a 100 mL volumetric flask and diluted with Ethanol.

Chromatographic separation

The Chromatographic separation was performed on thin layer chromatography (TLC) 10 cm x 20 cm aluminum plates coated with 0.2 mm layers of silica gel 60F254 (E. Merck, Darmstadt, Germany) with fluorescent indicator. Samples were applied to the plates. The origin and mobile phase line are marked using a soft pencil on silica gel 60 F²⁵⁴ layer (called a "chromatoplate"), and disposable 2 μ L glass micropipets are used to spot the standards and sample 1.5 cm up from the bottom edge. The bands were dried, then placed in a glass Jar and slowly solvated by a "mobile phase." The solvent used as mobile phase in the TLC was *n*-hexane: chloroform: methanol (1:7:2, v/v/v) for Combivir and *n*-hexane: chloroform: methanol (1:6:3, v/v/v) for Kaletra, after that linear ascending was developed for 25 min at room temperature (25°C).

The chromatoplate is removed, and the mobile phase is evaporated and was visualized under 254 nm ultraviolet (UV) light.

FTIR spectra of four drugs, namely Combivir, Kaletra, Valcyte and Viramune were analyzed by using Shimadzu SSU-8000 Fourier Transform Spectrophotometer by KBr disc method. The procedure consisted of dispersing a sample (drug alone) in KBr and compressing into disc by applying a pressure of 5 tons for 5 min in a hydraulic press. The pellet was placed in the light path and the spectrum was obtained by scanning at between 400 and 4,000 cm^{-1} .

FTIR Data for Combivir (Lamivudine- Zidovudine)

The characteristics peak of the hydroxyl group (OH stretching) at 3440.24 cm^{-1} a band peak at 3392.38 cm^{-1} owing amino group (NH_2 stretching), the characteristics peak of the carbonyl group ($\text{C}=\text{O}$ stretching) present in the cystidine nucleus at 1652.15 cm^{-1} , a band peak at 1454.66 cm^{-1} owing $\text{C}=\text{C}$ stretching (aromatic) confirm the presence of lamivudine. Peaks at 1278.23 and 1155.47 cm^{-1} owing to asymmetrical and symmetrical stretching of C-O-C system present in the oxathiolane ring.

For Zidovudine the characteristics peak of the hydroxyl group (OH stretching) at 3466.85 cm^{-1} a band peak at 2130.16 cm^{-1} owing azide group ($-\text{N}_3$ stretching), the carbonyl group ($\text{C}=\text{O}$ stretching) present in the amide group at 1681.55 cm^{-1} , a band peak at 1680.16 cm^{-1} owing imino group (N-H stretching), a band peak at 1465.16 cm^{-1} owing $\text{C}=\text{C}$ stretching (aromatic). One band in 1374 cm^{-1} is assigned to CH_2 . Peaks at 1279.51 and 1170.55 cm^{-1} owing to asymmetrical and symmetrical stretching of C-O-C system present in the oxalane ring.

FTIR Data for Viramune (Nevirapine anhydrate)

The FTIR spectrum of Nevirapine showed sharp characteristics peaks at N-H Stretching and $\text{C}=\text{O}$ at 3284.34 and 1654.58 cm^{-1} of cyclic amide of 7-membered ring in Nevirapine, respectively. Also C-H stretch peak at 2950.93 cm^{-1} and a band peak at 1450.49 cm^{-1} owing to $\text{C}=\text{C}$ stretching (pyridine ring).

FTIR Data for Valcyte (Valganciclovir hydrochloride)

The characteristics peak of the hydroxyl group (OH stretching) at 3443.27 cm^{-1} a band peak at 3395.30 cm^{-1} owing to amino group (NH_2 stretching), the characteristics

peak of the N-H stretching imino group at 3480.28 cm^{-1} , a band peak at 1730.58 cm^{-1} owing to carbonyl group of ester linkage but the characteristics peak of the carbonyl group ($\text{C}=\text{O}$ stretching) appear at 1663.64 cm^{-1} . Peaks at 1294.72 and 1152.89 cm^{-1} owing to asymmetrical and symmetrical stretching of C-O-C system.

FTIR Data for Kaletra (Lopinavir-Ritonavir)

The characteristics peak of the hydroxyl group (OH stretching) at 3436.22 cm^{-1} a band peak at 3399.33 cm^{-1} owing to imino group (N-H stretching), the characteristics peak of the carbonyl group ($\text{C}=\text{O}$ stretching) present in the amide group at 1653.35 cm^{-1} , a band peak at 1450.49 cm^{-1} owing to $\text{C}=\text{C}$ stretching (aromatic) confirm the presence of Lopinavir. Peaks at 1290.42 and 1150.82 cm^{-1} owing to asymmetrical and symmetrical stretching of C-O-C system.

For Ritonavir the characteristics peak of the N-H stretching amide group at 3484.82 cm^{-1} a band peak at 1723.18 cm^{-1} owing to the carbonyl group of ester linkage, the carbonyl group ($\text{C}=\text{O}$ stretching) present in the amide group at 1686.73 cm^{-1} . One band in 2964.35 cm^{-1} is assigned to hydrogen-bonded acid within the molecule. Peaks at 1645.87, 1621.57, and 1530.23 cm^{-1} owing to ($-\text{C}=\text{C}-$ stretching aromatic carbons) present in the benzene ring.

Results and discussions

The procedure of the optimal linear smoothing

The FTIR data obtained for four the above mentioned drugs represent themselves the random sequences depending on the wave length λ (cm^{-1}). In order to extract the reliable information we subject these data to the procedure of the optimal linear smoothing (POLS) [15] in order to eliminate the high-frequency fluctuations and extract the desired trend. We omit the details of this procedure because the POLS were described earlier in papers [15-17]. In order to decrease the influence of these fluctuations we applied this procedure to the curves that are obtained from the initial ones by numerical integration relatively its mean value. The usefulness of this procedure was demonstrated earlier in recent paper [18]. In the result of application of the POLS we obtain the smoothed trends that can be analyzed in terms of the Fourier transform.

The results of the application of the POLS are depicted on figures 1-8. Each couple of figures shows the desired trend (smoothed FTIR spectrum) and the dependence of the relative error with respect to the value of the current window.

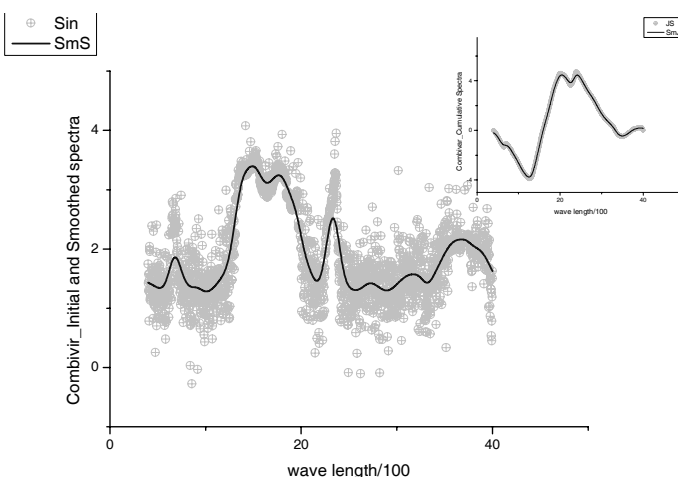


Fig. 1.

Figure 1 shows the results of application of the POLS procedure for FTIR spectra for the drug Combivir. In the right corner inside a small frame we show the result of the application of the POLS for the cumulative spectrum obtained from the initial one by numerical integration with respect to its mean value. As one can notice from this figure the cumulative spectrum is less “noisy” and the calculation of the value of the optimal smoothing window w_{opt} is facilitated considerably. The spectrum depicted by the solid line on the central figure is calculated at the same value w_{opt} that has been calculated initially for the cumulative spectra.

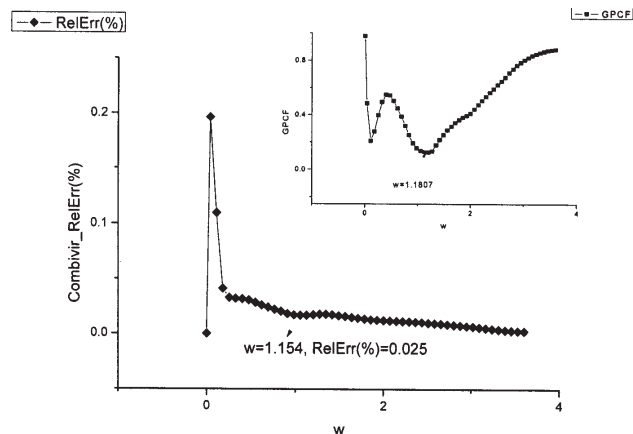


Fig. 2.

Figure 2 shows the behavior of the relative error for the drug Combivir with respect of the value of the smoothing window. The value of the smoothing window $w=1.154$ (corresponding to the first local minima) correlates with the minimal value of the function CCM $w=1.181$ when the high-frequency fluctuations are separated from the low-frequency ones.

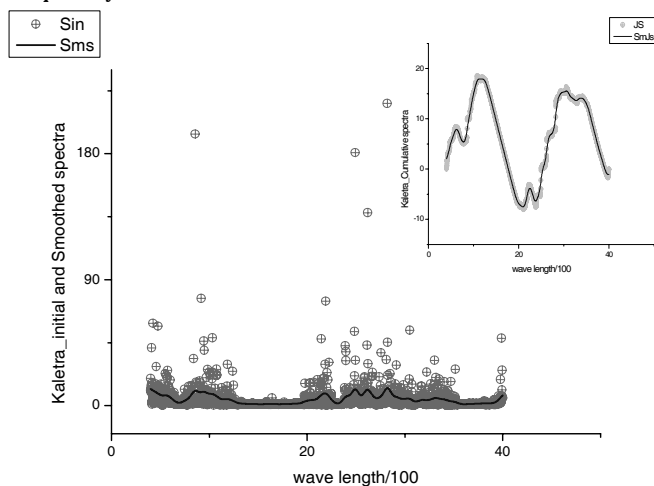


Fig. 3.

Figure 3 presented the initial FTIR spectra corresponding to Kaletra drug shown by magenta color. In order to decrease the influence of a “noise” the POLS is applied to the cumulative curve shown by light grey color inside a small frame. The value of the optimal smoothing window obtained for the cumulative curve is used for calculation of the optimal trend shown by solid blue line on the central figure.

The central plot shows the dependence of the relative error $RelErr(w)$ for the drug Kaletra. Again, the value of the smoothing window $w=0.445$ calculated for the cumulative curve correlates with the minimal value of the function CCM $w=0.458$ (depicted in the right corner inside the small frame) which differentiates the high-frequency fluctuations from the desired trend (fig. 4).

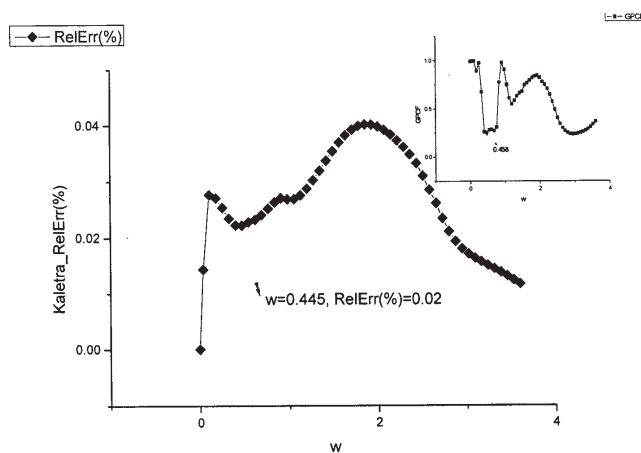


Fig. 4.

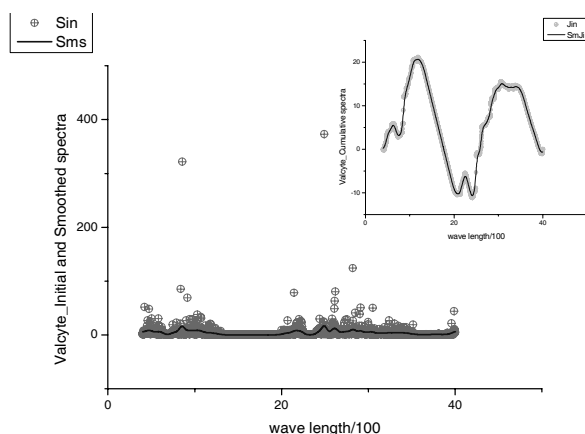


Fig. 5.

The initial FTIR spectra corresponding to the Valcyte drug is shown by magenta color. One can notice this spectrum is similar to FTIR (Kaletra) (fig. 5). The same POLS applied to the cumulative curve (shown in the right corner) leads to the smoothed light grey color cumulative spectrum. The value of the optimal smoothing window obtained for the cumulative curve is used for calculation of the optimal trend shown by solid blue line on the central figure.

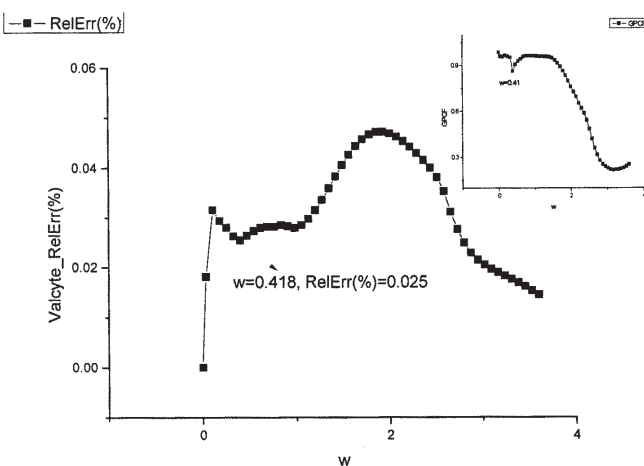


Fig. 6.

The central plot shows the dependence of the relative error for the drug Valcyte $RelErr(w)$. Again, the value of the smoothing window $w=0.418$ (fig. 6) calculated for the cumulative curve correlates with the minimal value of the function CCM $w=0.411$ (depicted in the right corner inside the small frame). As before this boundary point differentiates the high-frequency fluctuations from the desired trend.

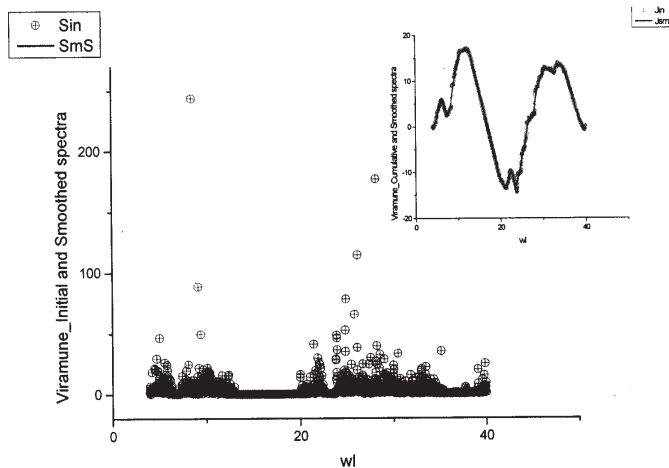


Fig. 7.

The FTIR spectra depicted on figure 7 corresponds to the Viramune drug and is shown by magenta color. One can notice that this spectrum is similar to the FTIR shown on Figs. 3 and 5. The same POLS applied to the cumulative curve (shown in the right corner) leads to the smoothed light grey color cumulative spectrum. The value of the optimal smoothing window obtained for the cumulative curve is used for calculation of the optimal trend shown by solid blue line on the central figure.

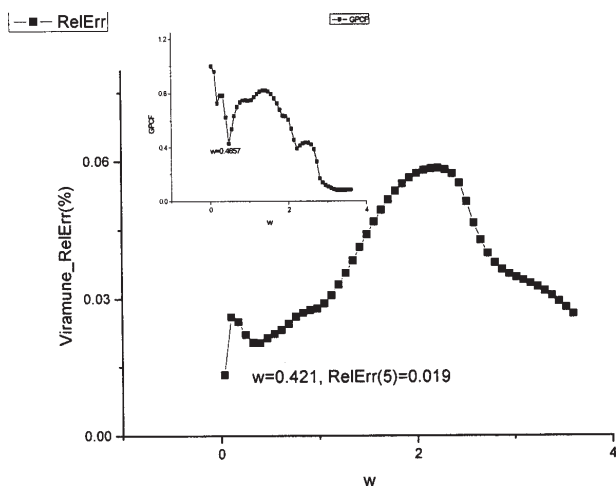


Fig. 8.

The central plot shows the dependence of the relative error for the drag Viramune $RelErr(w)$ (fig. 8). Again, the value of the smoothing window $w=0.421$ calculated for the cumulative curve correlates with the minimal value of the function CCM $w=0.457$ (depicted in the left corner inside the small frame). As before this boundary point differentiates the high-frequency fluctuations from the desired trend.

Usually the optimal value of the smoothing window is located in the interval $[\Delta/1000, \Delta/10]$, where Δ defines the relative length of the initial interval $\Delta = x_N - x_0$. For simplicity we use as the independent x variable the normalized value of the wavelength λ , i.e. $x = \lambda/100$. In order to have the independent criterion for verification of the value of the optimal smoothing window we used the behaviour of the generalized Pearson correlation function (GPCF). This function is considered in paper [18]. The GPCF (based on the statistics of the fractional moments [19]) was introduced previously in paper [20] and it is determined as

$$GPCF_p = \frac{GMV_p(1,2)}{\sqrt{GMV_p(1,1) \cdot GMV_p(2,2)}}, \quad (1)$$

where the generalized mean value function (GMV-function), in turn, is defined as

$$GMV_p(k,l) = \left(\frac{1}{N} \sum_{j=1}^N |nrm_j(k) \cdot nrm_j(l)|^{mom_p} \right)^{1/mom_p}$$

$$mom_p = \exp(Ln_p), \quad Ln_p = mn + \left(\frac{p}{P} \right) \cdot (mx - mn), \quad (2)$$

$$p = 0, 1, \dots, P$$

Here the values k and l numerate a couple of sequences compared. The normalized sequences located in the interval $0 < nrm(y) < 1$ are determined below by expression (3). The value mom_p determines the current moment from the interval $[0, P]$. The value P determines the final value of the function Ln_p located in the interval $[mn, mx]$. The values mn and mx define correspondingly the limits of the moments in the uniform logarithmic scale. In many practical cases these values are chosen as $mn = -15$, $mx = 15$ and P is chosen as integer value from the interval $[50, 100]$. This choice is related to the fact that the transition region of the random sequences considered expressed in the form of the GMV-functions are concentrated in the interval $Ln_p \in [-5, 5]$ and the extended interval $[-15, 15]$ is taken for showing the limiting values of this function in the space of moments. The initial sequences are chosen in that way: the minimum of the GMV-function coincides with zero value while the maximal value of this function coincides with $\max(nrm(y))$. In formula (2) the random sequences are supposed to be normalized to the unit value in accordance with expression

$$nrm_j(y) = \frac{y_j^{(+)} - y_j^{(-)}}{\max(y_j^{(+)}) - \min(y_j^{(-)})}, \quad y_j^{(\pm)} = \frac{1}{2} (y_j \pm |y_j|), \quad (3)$$

$$j = 1, 2, \dots, N, \quad 0 < nrm(y) < 1.$$

Here the set y_j defines the initial random sequence that can contain the trend or can be compared with another sequence without trend. The symbol $|...|$ and index j determines the absolute value and number of the measured points, correspondingly. If the limits mn and mx in (2) have the opposite signs and accept sufficiently large values then the GPCF function has two plateaus (equaled one at small numbers of mn (i.e. $GPCF_{mn} = 1$) and another limiting value $GPCF_{mx}$ depends on the degree of correlation between the random sequences compared. This right-hand limit (defined as L) is located between two values

$$M \equiv \min(GPCF_p) \leq L \equiv GPCF_{mx} \leq 1 \quad (4)$$

The appearance of two plateaus implies that all information about possible correlations is complete and further increasing of the limiting numbers (mx, mn) figuring in (7) is *not* necessary. The numerous test calculations show that the high degree of correlations between two random sequences compared is observed when $GPCF_{mx}$ coincides with the unit value, while the lowest correlations are observed when $GPCF_{mx}$ is equaled to its minimal value (M). This simple observation having general character for all random sequences allows us to introduce new correlation parameter CC (complete correlation) - factor, which is determined as

$$CC = \left(\frac{L}{M} \right) \cdot \left(\frac{L - M}{1 - M} \right). \quad (5)$$

We would like to stress here that this factor is determined on the *total* set of the fractional moments located between $\exp(mn)$ and $\exp(mx)$ values (see definition (2)). As it has been remarked above, in practical calculations for many cases it is sufficient to put $mn = -15$ and $mx = +15$, correspondingly. The upper row in (10) is referred to the CCL (with respect to the limiting value L) while the low row determines the factor associated with the minimal value M . In practical calculations, both factors are useful for analysis but the CCL-factor is less sensitive to the strong correlations (or small perturbations of the initial sequence) in comparison with the CCM. The CC-factor equals to unit value when the degree of correlation is high and the case $L = M$ corresponds to the lowest degrees of correlations that can be observed between the compared random sequences.

In addition, we want to stress also the following fact. This statistical parameter does *not* depend on the amplitudes of the random sequences compared. The pair random sequences compared should be normalized to the interval: $0 \leq |y| \leq 1$. It reflects the *internal* structure of correlations of the compared random sequences based presumably on the similarity of the probability distribution functions that are *not* known in many cases. In order to see how the high-frequency fluctuations are separated from the low-frequency fluctuations (which is usually defined as a trend) we put as initial function some FTIR spectrum $nrm_i(1) = \text{FTIR}(d)$ (d (Combivir, Kaletra, Valcyte, Viramune)). As a second sequence we use the smoothed spectra obtained at the fixed value of the window w_k from the interval $[w_{\min} = \Delta/1000, w_{\max} = \Delta/10]$. It is calculated as

$$y_j(2, w_k) = Gsm(x, y, w_k) \equiv \frac{\sum_{j=1}^N K\left(\frac{x_i - x_j}{w_k}\right) y_j}{\sum_{j=1}^N K\left(\frac{x_i - x_j}{w_k}\right)}, \quad K(x) = \exp\left(-\frac{x^2}{2}\right). \quad (6)$$

The normalized value $nrm_i(2)$ is obtained from $y_j(2, w_k)$ in accordance with expression (3). Then the value of the CCM(w_k) from (5) is calculated with respect to the value of the current window w_k . The results for each FTIR(d) spectra is presented on figures (2, 4, 6, 8), correspondingly. One can notice that the values of the relative error defined by expression (7) are strongly correlated with the minimal value of the CCM function. This boundary value $w_{\text{bound}} \approx w_{\text{opt}}$ separates the correlations evoked by high-frequency fluctuations from low-frequency ones. This observation helps to find some additional arguments that justify the selection of the optimal trend with accordance of expressions (7). That is why this trend can be defined as the *pseudo-fitting* function which divides the noise from a trend.

$$\tilde{y}_{w'} = Gsm(x, \tilde{y}_w, w'), \quad w' < w,$$

$$\min(\text{RelErr}) = \left[\frac{\text{stdev}(|y_w - y_{w'}|)}{\text{mean}(|y_w|)} \right] \cdot 100 \%,$$

$$\text{stdev}(y) = \left(\frac{1}{N} \sum_{j=1}^N (\Delta y_j)^2 \right)^{1/2}, \quad \Delta y_j = y_j - \text{mean}(y), \quad (7)$$

$$\text{mean}(y) = \frac{1}{N} \sum_{j=1}^N y_j.$$

The Fourier transform of the second type

In the context of this paper the Fourier transform of the second type is used as the fitting function based on some

significant set of “frequencies”. In accordance with conventional definition we determine this transformation of the second order as

$$\text{SmFTIR}(x_j; d) \equiv F(x_j) = A_0 + \sum_{k=1}^K \left[A c_k \cos\left(2\pi k \frac{x_j}{L}\right) + A s_k \sin\left(2\pi k \frac{x_j}{L}\right) \right],$$

$$\omega_k = 2\pi k \left(\frac{1}{L}\right) \quad (8)$$

We suppose that the characteristic inverse length L coincides with the maximal length of the interval $\Delta = x_N - x_0 = L$ and is measured in the same units as wavelength λ . If the value L is supposed to be known then the unknown decomposition coefficients $A c_k$ and $A s_k$ can be found by the linear-least square method (LLSM) and the limiting value K can be found from the condition of minimization of the value of the relative error

$$1\% < \text{RelErr} = \left[\frac{\text{stdev}(|\text{SmFTIR}(x_j, d) - F(x_j, K)|)}{\text{mean}(|\text{SmFTIR}(x_j, d)|)} \right] \cdot 100\% < 10\% \quad (9)$$

that should be located in the reasonable interval (1-10%). It is interesting to note that this new interpretation of the discrete Fourier transform as the fitting function of the initial signal does *not* coincide with conventional presentation of the Fourier transform as presentation of the function in the frequency space. The coefficients $A c_k$ and $A s_k$ found in the result of the application LLSM do not coincide with decomposition coefficients found in the result of application of the conventional program based on the fast Fourier transformation (FFT) and its modifications. The figures 9-12 demonstrate the results of the fit by the LLSM and figures 13-16 show the differences between the decomposition coefficients that are calculated from expression (8) and from the conventional program based on the fast Fourier transformation (FFT).

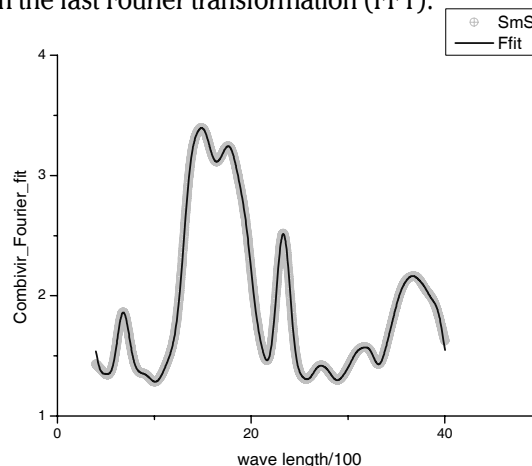


Fig. 9.

Figure 9 shows the fit of the smoothed spectra FTIR (Combivir) to the function (8). The values of the relative error (0.43%) and the value of the constant A_0 from (8) are collected in table 1. For the fitting of this curve with accuracy less than 1% only $K=35$ coefficients $A c_k$ and $A s_k$ are needed.

Figure 10 shows the fit of the smoothed spectra FTIR (Kaletra) to the function (8). The values of the relative error (4.02%) and the value of the constant $A_0 = 4.66789$ from (8) are collected in table 1. For the fitting of this curve with accuracy less than 5% only $K=35$ coefficients $A c_k$ and $A s_k$ are needed.

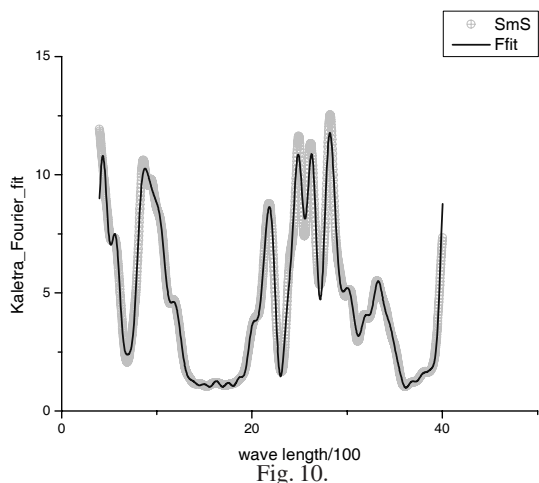


Fig. 10.

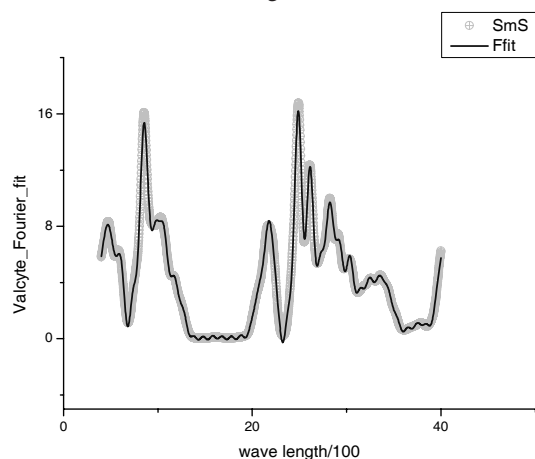


Fig. 11.

Figure 11 shows the fit of the smoothed spectra FTIR (Valcyte) to the function (8). The values of the relative error (5.16%) and the value of the constant $A_0 = 4.18415$ from (8) are collected in table 1. For the fitting of this curve with accuracy close to 5% only 35 coefficients Ac_k and As_k are needed. We want to stress here that the fitting parameters of this spectrum is close to the FTIR (Kaletra).

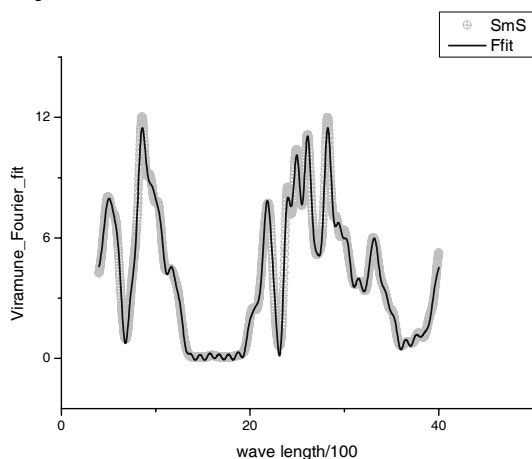


Fig. 12

Figure 12 shows the fit of the smoothed spectra FTIR (Viramune) to the function (8). The values of the relative error (5.01%) and the value of the constant $A_0 = 4.06988$ from (8) are collected in table 1. For the fitting of this curve with accuracy close to 5% only 35 coefficients Ac_k and As_k are needed. One can notice that this spectrum is similar to the smoothed spectra calculated for Kaletra and Valcyte drugs, correspondingly.

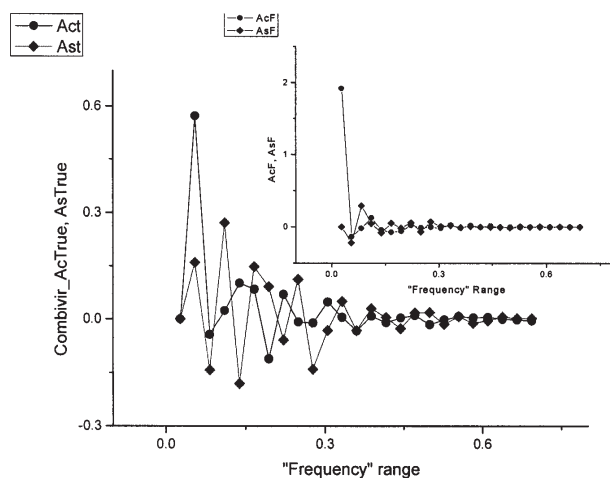


Fig. 13.

Here we show the distribution of the coefficients Ac_k and As_k for the spectrum Combivir depicted on figure 9. They are calculated in the frame of the LLSM. For comparison in the small frame we give the distribution of the coefficients AcF_k , AsF_k obtained with the help of the conventional program. One can notice that they are different (fig. 13).

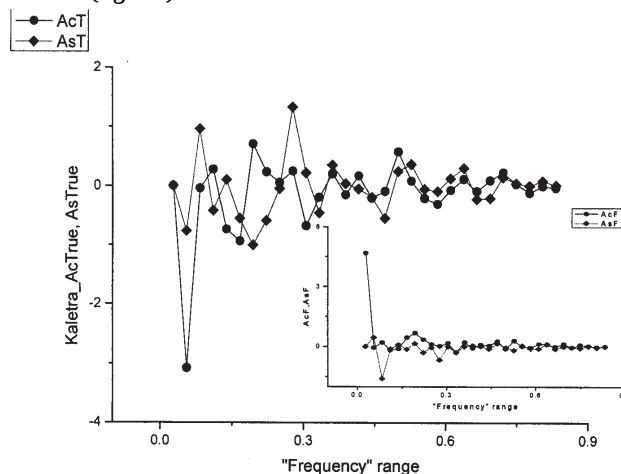


Fig. 14.

Here we show the distribution of the coefficients Ac_k and As_k for the spectrum Kaletra depicted on figure 10. These decomposition coefficients are calculated in the frame of the LLSM. For comparison in the small frame below we give the distribution of the coefficients AcF_k , AsF_k obtained with the help of the conventional program. One can notice that they are different (fig. 14).

The drug name	K	L	A_0	RelErr(%)	PCC
Combivir	25	36.0337	1.91856	0.430045	0.999918
Kaletra	35	36.0337	4.66789	4.02807	0.998182
Valcyte	35	36.0337	4.18415	5.16648	0.998259
Viramune	35	36.0337	4.06988	5.01071	0.998014

Table 1

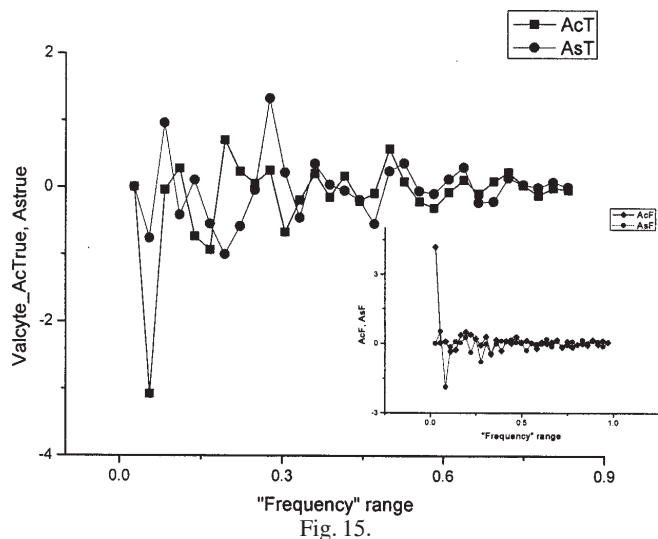


Fig. 15.

In figure 15 we show the distribution of the coefficients Ac_k and As_k for the spectrum Valcyte depicted on figure 11. The distribution of the coefficients is calculated by means of the LLSM. For comparison in the small frame below we give the distribution of the coefficients AcF_k , AsF_k obtained with the help of the conventional program. One can notice again that these decomposition coefficients in comparison with the coefficients obtained by means of the LLSM are different.

In figure 16 we show the distribution of the coefficients Ac_k and As_k for the spectrum Viramune depicted on figure 12. In the small frame below we give the distribution of the coefficients AcF_k , AsF_k obtained with the help of the conventional program. One can notice again that these decomposition coefficients in comparison with the coefficients obtained by means of the LLSM are different.

In the first column of table 1 we give the values of the last mode that enters to the decomposition (8). The second and the third columns show correspondingly the values of the L and the coefficient A_0 . The last 4 and 5 columns demonstrate the parameters of the fitting procedure: the value of the relative error (defined by expression (9)) and the Pearson correlation coefficient (PCC).

Conclusions

We conclude that the analysis of the FTIR spectra corresponding to our four investigated drugs can be based on the analysis of the amplitude-“frequency” responses (AFR) (we notice that in our case “frequency” coincides with the value $\omega_k = 2\pi k/L$. This set of the “frequencies” giving the acceptable accuracy should be located in the interval $[\omega_{\min} = 2\pi/L, \omega_{\max} = 2\pi K/L]$. So, we show that new consideration of the Fourier transform (used as a fitting function of the initial signal) gives new possibilities for the interpretation of the smoothed FTIR data in terms of reduced set of the calculated amplitudes Ac_k and As_k . The figures 13-16 represent the final results of this new signal analysis.

The results obtained in this manuscript strongly encourage us to use this error controlled procedure for the quality control of the commercial samples of compounds.

Acknowledgements: This work was funded by the Deanship of Scientific Research (DSR), King Abdulaziz University, Jeddah, under grant No. Gr/34/11. The authors, therefore, acknowledge with thanks DSR technical and financial support. One of us (RRN) wants to stress that this work was realized partly in the frame of the program “Dielectric spectroscopy and signal/noise analysis of complex systems”. This scientific program was accepted by Kazan federal university for the period 2012-2014 years.

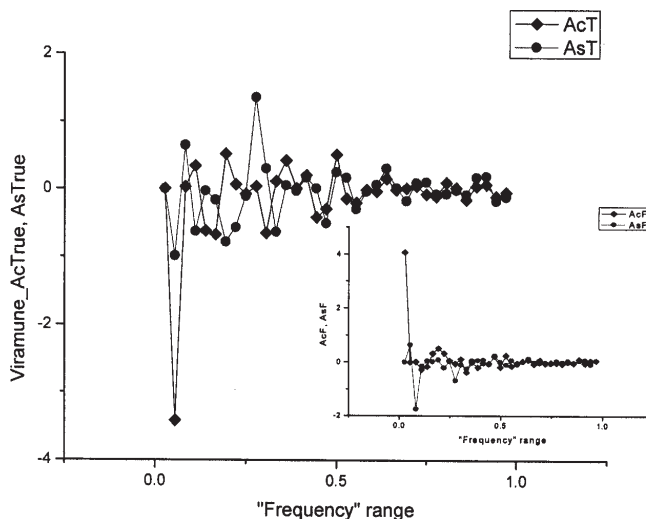


Fig. 16.

References

1. KLAFTER J., LIM S. C., METZLER R. (Eds.), Fractional Dynamics in Physics: Recent Advances, World Scientific, Singapore, 2011.
2. DAUBECHIES I., Ten Lectures on Wavelets, SIAM, Philadelphia, Pennsylvania, 1992.
3. SABATIER J., AGRAWAL O. P., MACHADO J.A. T. (Eds.), Advances in Fractional Calculus: Theoretical Developments and Applications in Physics and Engineering, Springer, Dordrecht, 2007.
4. NIGMATULLIN R. R., IONESCU C. M., OSOKIN S.I., BALEANU D., TOBOEV V.A., Rom. Rep. Phys., 2012, **64**(4), p. 1032.
5. DINC E., BALEANU D., Rev. Chim.(Bucharest), **60**, no. 8, 2009, p. 741.
6. DINC E., BALEANU D., Comput. Math. Appl., 2010, **59**(5), p. 1701.
7. KAMBUR M., IBRAHIM N., DINC E., BALEANU D., Rev. Chim.(Bucharest), **62**, no. 6, 2011, p. 618.
8. *** UNAIDS. Report on the global AIDS epidemic 2008.
9. SIMON C., EVERITT H., BIRTWISTLE J., STEVENSON B., Oxford Hand Book of General Practice, Infective Disease, Human Immunodeficiency Virus, Oxford University Press, New Delhi, India, 2002.
10. *** WHO public assessment report, Abacavir Sulfate, Lamivudine and Zidovudine Tablets 300mg/150mg/300mg. 2009;Part 7:1-2.
11. MANOSUTHI W., THONGYEN S., NILKAMHANG S., MANOSUTHI S., SUNGANUPARPH S., AIDS Research and Therapy 2012, 9:8.
12. CURRAN M., NOBLE S. Drugs 2001, **61**, p.1145; MARTIN, J. C., TIPPIE, M. A., MCGEE D. P. C., VERHEYDEN J. P. H., J. Pharm. Sci. **1987**, 76, 180; Steininger, C.Recent Patent. Anti-Infect. Drug Discover. 2007, **2**, p. 53.
13. *** Annex, Proposal to waive in vivo bioequivalence requirements for WHO Model List of Essential Medicines immediate-release, solid oral dosage forms WHO Technical Report Series, 2006, **937**, p. 413.
14. RICHMAN D.D., MARGOLIS D.M., DELANEY M., GREENE W.C., HAZUDA D., POMERANTZ R.J., Science, 2009, **323**, p.1304.
15. PERSHIN S.M., BUNKIN A. F., LUKYANCHENKO V.A., NIGMATULLIN R. R., Lazer Phys.Lett., 2007, **4** (11), p. 809.
16. BALEANU C.M., NIGMATULLIN R.R., CETIN S.S., BALEANU D., OZCELIK S., Centr. Eur. J. Phys., 2011, **9**(3), p 729.
17. CIUREA M. L., LAZANU S., STAVARACHER I., LEPADATU A.M., IANCU V., MITROI M. R., NIGMATULLIN R. R., BALEANU C.M., J. Appl. Phys., 2011, **109**, p. 013717.
18. NIGMATULLIN R. R., IONESCU C., BALEANU D., J. Sign., Imag. Video Proc., 2012, DOI:10.1007/s11760-012-0386-1.
19. NIGMATULLIN R. R., J. Sign. Proc., 2006, **86**, p 2529
20. NIGMATULLIN R. R., ARBUZOV A.A., NELSON S. O., J. Instrum. (2006) JINST, N1-P10002.

Manuscript received: 22.04.2013